e-ISSN: 2687-6698 **Research Article**

Turkish Journal of Analytical Chemistry
TurkJAC
www.turkjac.org
2019

The relationship between hydrothermal alteration and element accumulation in sessile oak (*Quercus petraea L.*): A case study from the Canca hydrothermal alteration zone (Gümüşhane, Türkiye)

Alaaddin Vural

Ankara University, Faculty of Engineering, Department of Geological Engineering, 06830, Ankara, Türkiye

Abstract

The aim of this study is to investigate the element accumulation capability of sessile oak trees, specifically focusing on their ability and characteristics to accumulate trace elements in the context of plants/trees in alteration zones. The Canca hydrothermal alteration zone (Gümüşhane, Türkiye) is located in Gümüşhane, one of Türkiye's significant mining provinces, which hosts numerous mineralizations. The area has been subjected to intense hydrothermal alteration, making it particularly notable for signs of precious and base metal mineralization. Sessile oak (*Quercus petraea L.*) leaves were collected from the Canca hydrothermal alteration zone, and their analyses were conducted using an ICP-MS device. The trace element concentrations in the oak leaves were evaluated geostatistically, and the element distributions in the Canca area were examined using element distribution maps created by spatial geostatistical methods. When the findings were collectively evaluated, it was determined that the trace element contents in the sessile oak leaves were generally higher than normal element contents, associated with the alteration in the area. Notably, a more significant enrichment of Mo (from 0.05 to 5.47 ppm, with a median value of 0.71 ppm), Cu (from 2.85 to 14.64 ppm, with a median value of 5.97 ppm) As (from 0.01 to 1.36 ppm, with a median value of 0.14 ppm), Zn (from 7.37 to 52.53 ppm, with a median value of 19.15 ppm) and Pb (from 0.29 to 2.23 ppm, with a median value of 0.83 ppm) elements was found to be related to the alteration. In addition, a slight enrichment by other elements (Cr, Mn, Co, Ni, Sb and Ba) has been detected. As a result, this study contributes to the related literature by elucidating the elemental accumulation pattern and alteration relationship of sessile oak leaves grown in the alteration zone associated with mineralization.

Keywords: Biogeochemistry, element accumulation, exploration geochemistry, hydrothermal alteration, trace elements

1. Introduction

The geochemical properties of elements and their mobility in different environments are among the many factors influencing element accumulation in plants [1–5]. Therefore, the use of plants for geochemical prospecting in mineral exploration began in the 1950s, yielding satisfactory results from these studies. Such biogeochemical studies have contributed to the discovery of many mineral deposits during that period. Today, exploration geochemistry continues to utilize the element accumulation capabilities of plants.

The geochemical properties of elements, along with various physicochemical factors such as pH and Eh, and their mobility in different environments, significantly influence element accumulation in plants [2,6,7]. Therefore, the use of plants for geochemical prospecting in mineral exploration began in the 1950s, and these studies have yielded satisfactory results. Such biogeochemical studies contributed to the discovery of many mineral deposits during that period. Today, exploration geochemistry continues to benefit from the element accumulation capabilities of plants.

The Gümüşhane region has been the site of numerous mining activities since ancient times [8]. During the Republic period, exploration efforts in the region led to the discovery of many mineral deposits, which were subsequently developed for the national economy through the efforts of both the private sector and public institutions such as the General Directorate of Mineral Research and Exploration (MTA). The Canca (Gümüşhane, Türkiye) hydrothermal alteration zone, where the oak leaves were collected (Fig. 1), is part of the Eastern Black Sea Tectonic Belt, which forms a section of

Citation: A. Vural, The relationship between hydrothermal alteration and element accumulation in sessile oak (Quercus petraea L.): A case study from the Canca hydrothermal alteration zone (Gümüşhane, Türkiye), Turk J Anal Chem, 6(2), 2024, 61–70.
https://doi.org/10.51435/turkjac.1494920

Author of correspondence: alaaddinvural@hotmail.com
Tel: +90 (312) 203 3402
Fax: +90 (312) 215 04 87

Received: June 4, 2024
Accepted: June 27, 2024

the 6000 km long metallogenic belt extending from the Balkans to the Himalayas [9,10].

The region, situated at the transition between the Black Sea Climate and Continental climate, boasts a rich diversity of flora. Considering the mining potential of the region and its diverse plant life, it is evident that phytogeochemical studies conducted in the area would significantly contribute to mineral exploration efforts. Such studies are also crucial for investigating the element accumulation capabilities of plants in hydrothermal alteration and mineralization areas. Therefore, the Canca hydrothermal alteration zone, characterized by intense hydrothermal alteration and a dense sessile oak (*Quercus petraea* L.) forest, was selected as the target area for this study. A biogeochemistry/phytogeochemical study was conducted in the area to examine the relationship between the element accumulation capability of oak trees and hydrothermal alteration.

2. Materials and methods

2.1. Geological and Geographical Characteristics of the Region

The Canca hydrothermal alteration zone exhibits a rugged topography characterized by deep valleys and high peaks because of its geological and geotectonic history. The region experiences a transitional climate between a continental climate, characterized by hot and dry summers, and a Black Sea climate, characterized by cold and snowy winters.

The Canca area has been subjected to intense hydrothermal alteration due to the influence of Upper Cretaceous-Eocene magmatism. Considering the study

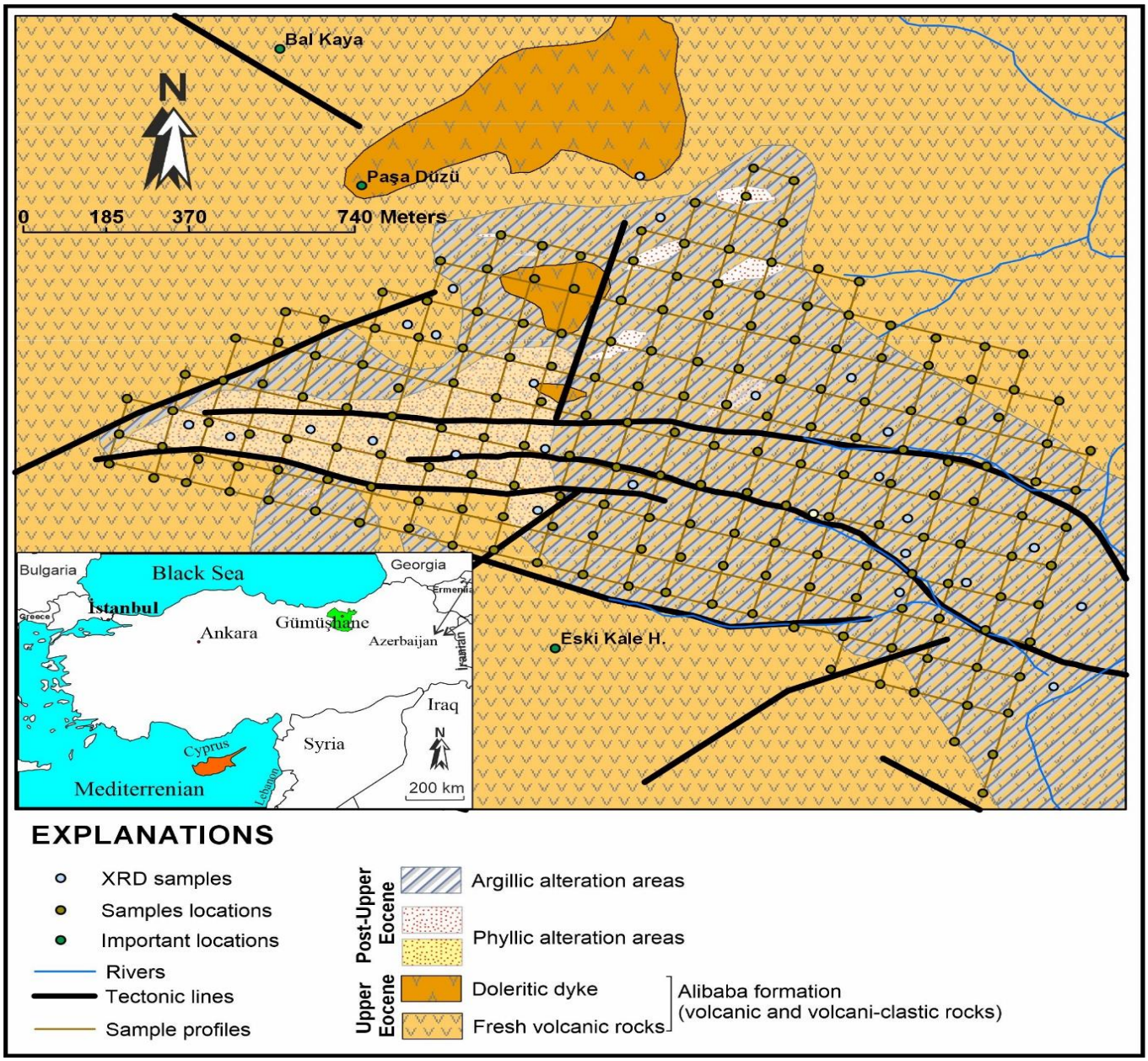

Figure 1. Geological and alteration map of the Canca (Gümüşhane, Türkiye) field [3]

area and its immediate surroundings, the primary rocks of the region consist of metamorphic rocks of the Eastern Black Sea Tectonic Belt and unmetamorphosed granitic plutons intruding them [11–13]. These primary rocks are unconformably cut by Early-Middle Jurassic volcaniclastic rocks (Zimonköy Formation) [14]. The Zimonköy Formation, in turn, is overlain by Late Jurassic-Early Cretaceous carbonate rocks (Berdiga Formation) [15]. The Berdiga Formation is covered by the Late Cretaceous Kermutdere Formation [16]. All of these units are intruded by Late Cretaceous intrusions on the northwest and southwest sides of Gümüşhane, near Torul [17,18]. In different locations northeast and southwest of Gümüşhane, Late Cretaceous volcanics overlay the formations. The Late Cretaceous sedimentary/volcanic/volcano-clastic units are overlain by Eocene volcanic and volcano-clastic units and intruded by coeval granitic rocks [9,19–22].

In the Canca area, the oldest unit is composed of Eocene volcano-clastic rocks (Fig. 1) [23]. These rocks have undergone intense hydrothermal alteration. The alteration in the area is predominantly characterized by argillic and phyllic alteration, and as a result of alteration, a well-developed soil cover of grayish, light brown podzolic type is commonly observed on the surface [4,24]. The youngest units in the region consist of recent travertine, alluvium, and slope debris [25].

2.2. Sample collection, analysis processes, and data evaluation

Sampling was conducted using sessile oak leaves due to the dense oak forest observed in the Canca hydrothermal alteration zone for biogeochemical purposes. A total of 226 plant samples were collected. Sample collection took place within the months of June and July in 2014, and the details of the sampling and analysis processes are provided in in Vural [3].

The analyses of oak leaves were carried out at the Central Laboratory of Gümüşhane University using an ICP-MS device (Agilent 7700x ICP-MS, Santa Clara, California, USA). Many elements were measured in sessile oak leaves as part of a project, however, this study focused on Cr, Mn, Fe, Co, Ni, Cu, Zn, As, Sr, Mo, Cd, Sb, Ba, and Pb.

All the chemicals used were analytical reagent grade and were bought from Merck (Darmstadt, Germany). Standard solutions were prepared to construct calibration graphs in ICP-MS by diluting the stock solution with 1000 mg/L concentrations of each metal in appropriate proportions. Polypropylene bottles were used to store standard solutions. Before usage, the vials were immersed in 10% nitric acid overnight, washed with ultrapure water, and finally dried.

The sessile oak leaves were ground into powder. Approximately 0.5 g of the powder samples were weighed and placed in Teflon vessels in a high-pressure and closed-coated microwave oven (Sineo MDS-8, Shanghai, China). After 7 mL of HNO_3 and 3 mL of H_2O_2 were added to the beakers, the contents were digested for approximately 30 minutes. Completely solubilized limpid solutions were finally quantitatively made up to 50 mL with distilled/deionized water and analyzed for the metals they contained by ICP-MS (Inductively Plasma – Mass Spectrometer) and MP-AES (Microwave Plasma – Atomic Emission Spekctrometer). Metal concentrations measured in mg/L units in the devices were then converted to mg/kg (ppm) units with Formula 1 [26,27].

$$\text{Concentration (mg/kg, ppm)} = \frac{C \times V \times S}{m} \quad (1)$$

Where, C is the mg/L concentration value measured in aqueous solution in the devices, V is the final volume (mL) completed after microwave solubilization, m is the weighed sample mass (g), and S is the dilution coefficient.

Accuracy/precision tests for the analyses were conducted according to relevant analysis procedures. To test the accuracy of the measurement method, standards of known concentrations were added to the samples at three consecutive levels. Concentrations of spiked samples were measured again by ICP-MS. Recovery percentages for added standard concentrations were calculated from the differences between the measurement results of the sample with spiked standard and the measurement results of the original sample without spiked standard. Spiked/recovery test results were between 92.8–108.0% satisfactory for all metals.

Another accuracy test was conducted by analyzing a certified reference material. The certified results and the measurements taken in this study with ICP-MS were found to be in very good agreement.

Relative standard deviations (RSD) were evaluated for the precision of metal measurements by ICP-MS. The standard deviation of each metal was divided by its average, and the result was multiplied by 100 to calculate the percent RSDs. From the results obtained, it was observed that RSD values varied between 0.7 and 2.8%.

Descriptive statistical parameters for element concentrations were calculated, and the distribution characteristics of the concentrations were attempted to be understood through statistical methods. Since the element contents of oak leaves did not follow a perfect normal distribution, average element concentrations were determined considering median values in an effort to reduce the influence of outliers. Threshold values for

Table 1. The instrumental conditions used for XRD analyses

Anode	Cu (CuKα =1.541871 Å)
Filter	Ni
Voltage	35 kV
Goniometer Speed	2°/minute
Paper Speed	2 cm/min
Sensitivity	4.102
Time Constant	1 sn
Slits	1°-0.1mm-1°
Paper Interval	TK 2θ = 2–70°, KF 2θ = 2–40°

the elements were determined by adding 2 median absolute deviations (MAD) to the median values [4]. To examine the effect of alteration on oak element accumulation, XRD analyses were conducted considering the alteration patterns in the field, aiming to characterize mineral assemblages typical of alteration suites. XRD analyses were performed at the Mineralogy Petrography Service of the General Directorate of Mineral Analysis and Technology of the MTA. The instrumental conditions used for XRD examinations are summarized in Table 1. In XRD studies, predominantly soil samples, and a small amount of altered rock samples have been used.

3. Results

When evaluating the element concentrations in sessile oak leaves (Cd and Sb in ppb, others in ppm), it was found that Cr concentrations ranged from 0.21 to 8.4 ppm, with a median value of 1.86 ppm. Similarly, Mn ranged from 13.6 to 1374.2 ppm (median: 162.8 ppm), Fe from 50.19 to 990.05 ppm (median: 317.6), Co from 0.05 to 0.89 ppm (median: 0.15 ppm), Ni from 0.33 to 8.75 ppm (median: 2.77 ppm), Cu from 2.85 to 14.64 ppm (median: 5.97 ppm), Zn from 7.37 to 52.53 ppm (median: 19.15 ppm), As from 0.01 to 1.36 ppm (median: 0.14 ppm), Mo from 0.05 to 5.47 ppm (median: 0.71 ppm), Cd from 6.84 to 249.5 ppb (median: 30.21 ppb), Sb from 10.96 to 2364 ppb (median: 95.1 ppb), Ba from 11.5 to 387.34 ppm (median: 113.35 ppm), and Pb from 0.29 to 2.23 ppm (median: 0.83 ppm) [4]. Compared to the literature data from samples collected in areas unaffected by hydrothermal alteration, these concentrations indicate an enrichment in especially Cr, Mn, Co, Ni, Cu, Zn, As, Mo, Sb, Ba, and Pb [3,28].

Based on XRD data and field observations, three types of alteration have been identified in the area: silicification, characterized by pervasive sericitization and pyritization, accompanied by hematite and limonite formations (silicification - phyllic alteration) (Fig. 1 and Fig. 2); argillic alteration, which includes kaolinite, illite, smectite, and alunite (Fig. 1 and Fig. 3). The argillic alteration surrounds the silicified zones and is widespread throughout the field. Silicification is predominantly associated with tectonic lines and fractures, observed

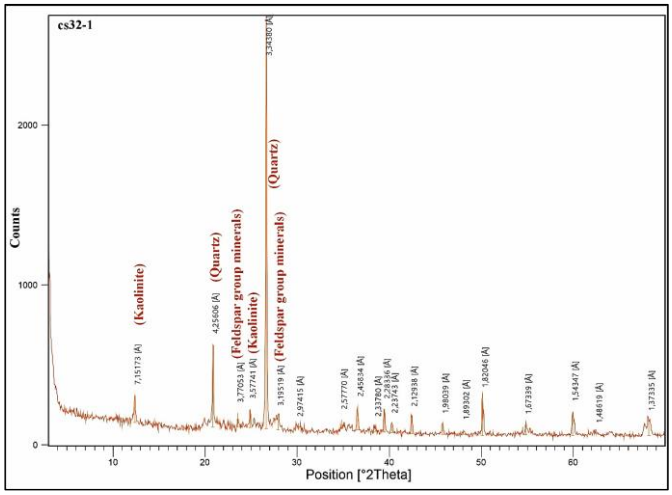

Figure 2. XRD pattern of the silicification-phyllic alteration zone

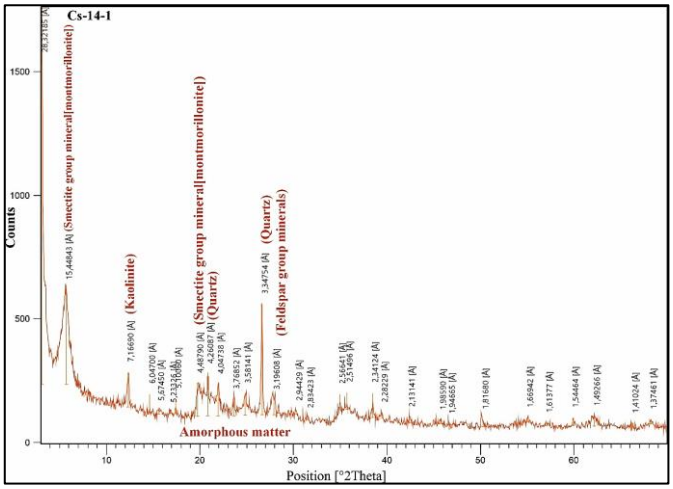

Figure 3. XRD patterns of the zones with intense argillic alteration

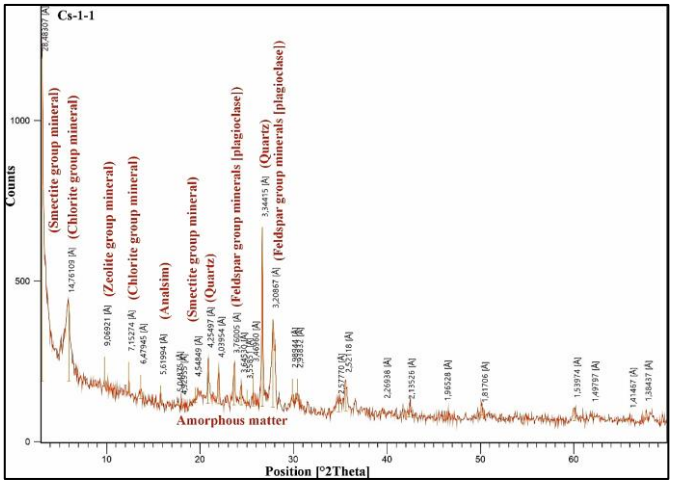

Figure 4. XRD patterns of the propylitic alteration areas

mainly in the western and eastern parts of the area in the phyllic zones (Fig. 1 and Fig 4). These silicified zones are primarily developed due to hydrothermal effects and are influenced by plutonic processes, indicating that mineralizations are likely to develop in these alteration zones.

Argillic alteration areas are predominantly influenced by weathering, developing supergene and indicating lower temperature effects, transitioning to

Table 2. Correlation coefficients (Spearman's rho) between elements in sessile oak leaves

	Cr	Mn	Fe	Co	Ni	Cu	Zn	As	Sr	Mo	Cd	Sb	Ba	Pb
Cr	1.000													
Mn	0.380	1.000												
Fe	0.964	0.412	1.000											
Co	0.662	0.589	0.698	1.000										
Ni	0.518	0.659	0.475	0.544	1.000									
Cu	0.602	0.045	0.641	0.452	0.136	1.000								
Zn	0.250	-0.007	0.286	0.235	-0.047	0.677	1.000							
As	0.627	0.176	0.782	0.482	0.070	0.588	0.325	1.000						
Sr	0.384	-0.065	0.497	0.245	0.063	0.586	0.332	0.632	1.000					
Mo	0.735	0.208	0.816	0.484	0.187	0.639	0.312	0.846	0.707	1.000				
Cd	0.176	0.420	0.228	0.481	0.326	0.312	0.496	0.115	0.019	0.027	1.000			
Sb	0.751	0.464	0.741	0.671	0.394	0.476	0.281	0.456	0.347	0.557	0.307	1.000		
Ba	0.026	0.060	0.003	-0.183	0.212	0.032	-0.116	-0.080	0.303	0.083	-0.188	-0.101	1.000	
Pb	0.548	0.291	0.681	0.551	0.232	0.600	0.507	0.783	0.528	0.651	0.479	0.405	0.048	1.000

propylitic alteration with a lower degree of hydrothermal alteration (Fig. 1 and Fig 4). Propylitic alteration areas predominantly consist of chlorite minerals, smectite group clay minerals, and a small amount of zeolite group minerals. These areas are the least affected by hydrothermal alteration, with weathering also contributing to the alteration. These zones exhibit minimal ore formation and element enrichment.

The relationship between the element contents of sessile oak leaves was examined by calculating the Spearman's rho nonparametric correlation coefficient (Table 2). The Spearman correlation coefficients (Spearman's rho) between the elements in sessile oak leaves indicate the strength and direction of the monotonic relationships between pairs of elements. Positive values suggest a positive correlation, where higher concentrations of one element are associated with higher concentrations of another, while negative values suggest an inverse relationship. Values closer to 1 or −1 indicate stronger correlations.

According to the correlation coefficients, a significant correlation was observed between Cr and Fe, Co, Ni, Cu, As, Mo, Sb, and Pb. Additionally, a notable correlation can be noted between Mn and Co, Ni, suggesting that Mn, Co, and Ni exhibit similar geochemical behaviors, indicating the influence of environmental/parental rock factors in this relationship. Spearman correlation coefficients also reveal a significant correlation between Co and Sb and Pb. Furthermore, a substantial correlation relationship is evident between Cu and As, Sr, Mo, and Pb elements. Moreover, significant correlations are observed between Zn and Cd, Pb; As and Mo, Pb; Mo and Sb, Pb; and Cd and Pb.

3.1. The spatial distributions of plants

Spatial distribution maps of element concentrations in oak leaves were plotted to examine the behavior of elements in relation to the geological environment (Fig. 5). The kriging method was employed in the generation of distribution maps [29], and the spatial weights of sample points were calculated using the variogram method [30]. The variogram function (γ (h)) expresses the variance of differences between two randomly separated variables as a function of distance. The semivariogram function is half of the variogram function and is computed by the following equation.

$$\gamma(h) = \frac{1}{2N(h)} \sum_{i=1}^{N(h)} [(x_i) - z(x_i + h)]^2 \quad (2)$$

Here, h denotes the lag distance, $\gamma(h)$ semivariogram, N(h) corresponds to pairs of sample points associated with distance h (Krige, 1951; Matheron, 1963; Yaylalı-Abanuz et al., 2011). Lag distance and $\gamma(h)$ semivariogram are plotted on the semivariogram graph. The purpose is to draw the most appropriate theoretical semivariogram for the experimental semivariogram. The kriging technique facilitates the estimation of variations at unsampled points with close accuracy using the structural components obtained from semivariograms. The kriging value is calculated using the following formula:

$$Z^*(x_o) = \sum_{i=1}^{n} \lambda_i Z(x_i) \quad (3)$$

Here, $Z^*(x_o)$: represents the unknown and estimated value at point (x_o), $Z(x_i)$ is the data used in the estimation at point (x_o), and λ_i is the weight assigned to these data. The values of variables at points $(x_i) = 1$ are known, but the weights assigned to them need to be calculated. In the kriging method, these weights should be defined such that the average of the predicted errors is zero and the variance is minimized. The conditions for optimality are expressed as follows:

$$E[Z(x_o) - Z^*(x_o)] = 0 \quad (4)$$

To minimize the variance of the prediction error, the variance $E[Z(x_o) - Z^*(x_o)]$ must be minimized. For interpolation to be unbiased, the sum of weights $\sum_{i=1}^{n} \lambda_i = 1$, thereby deriving n unknowns and n+1 equations. If the multipliers are solved using the Lagrange method, the number of equations equals the number of unknowns.

$$\sum_{i=1}^{n} \lambda_i \gamma(x_i - x_j) - m = \gamma(x_0 - x_j) \quad (5)$$

Where m is the Lagrange multiplier and γ is the variogram value for the distance between points $x_i$and x_j. The kriging variance is solved from the following equation:

$$\sigma^2 = \sum_{i=1}^{n} \lambda_i \gamma(x_i - x_j) - m = \gamma(x_0 - x_j) \quad (6)$$

Due to its superiority in providing the best linear system of equations for interpolation compared to other techniques, the kriging method is preferred more often (It should also be noted that the inverse distance weighting (IDW) method does not differ significantly from the kriging method). Therefore, the kriging method was applied to the elements Cr, Mn, Fe, Co, Ni, Cu, Zn, As, Sr, Mo, Pb, Cd, Sb, Ba and Pb using data obtained from the semivariogram model (Fig. 5). For the preparation of anomaly maps, the ARCGIS 10.8 program, which is developed for such studies and efficiently applies the theory of semivariogram and kriging method, was utilized. During the drawings, the spherical model of the kriging method was found to be the most suitable, and it was preferred to smooth out the roughness in the maps created by the kriging method. The element distribution maps were also created using the IDW method for the same elements. In general, no significant difference was observed in the distribution maps.

When examining the element distribution maps of sessile oak leaves, it is observed that chromium (Cr) distributions are concentrated in the west, northeast, and east of the field center in the west-east direction. Elevated Cr values were detected in the leaves of trees growing in areas with argillic alteration zones and fresh volcanic rocks transtion. Contrary to expectations, lower Cr concentrations were found in areas where dolerite rocks surfaced (Fig. 5).

Mn values are mostly found in the western part of the field within the argillic alteration zone and near the phyllitic zone. Additionally, high Mn values are observed in a small area in the east of the field within the argillic alteration zone. These enrichments are also thought to be related to tectonism. This is because the higher Mn values along the tectonic line are striking (Fig. 5).

Fe concentrations are high towards the southeast in the center of the field, which is also consistent with the main tectonic line. The distribution of Fe concentrations in the field is not uniform, but it shows a similar pattern to the distribution of Mn. High Fe concentrations are also relatively concentrated within the argillic alteration zone (Fig. 1 and Fig 5).

High Co values are observed in the northeastern part of the field, especially in areas with fresh rocks. Considering the association of high Co concentrations with alteration, it can be said that areas with both argillic and phyllic alteration zones (for the region in question) exhibit high values. For the western and southern parts of the field, high values are more likely associated with argillic alteration (Fig. 5).

The Ni concentrations in oak leaves also show relatively parallel distributions with Mn. High Ni distributions were observed mainly in areas with fresh rocks and in areas subjected to argillic alteration (Fig. 5).

Cu concentration distributions are higher in the northern and eastern parts of the field, within the argillite zone, compared to other parts of the region. The association of Cu enrichments in the eastern section with tectonic faults is also striking. While Zn concentrations overlap with Cu in some points, there is an inverse relationship in some areas, as seen from the distribution maps (Fig. 5 and Fig. 6). Zn enrichments (in the eastern part of the field) are associated with tectonic faults and argillic alteration (Fig. 6).

As distributions are concentrated in a limited area in the field and intensify towards the northwest-southeast direction from the center of the field. The intensification is mainly observed within the argillic zone and tectonic lines.

A high Sr element distribution was also observed in the eastern part of the field where there is tectonic intensity and intense alteration (especially argillic alteration) (in the range of 200370 ppm). In the areas where fresh rocks are exposed, the Sr element exhibits a distribution pattern of small values (in the range of 12–31 ppm) (Fig. 6).

Concentrations of Mo are concentrated in a limited area of the field and in the northern part within the argillic-phyllic transition zone (Fig. 6). It is also observed that Mo distributions relatively overlap with As distributions.

The Cd distributions in the field are mostly found in fresh rocks and relatively in the argillic alteration zones (up to in the range of 120–250 ppb).

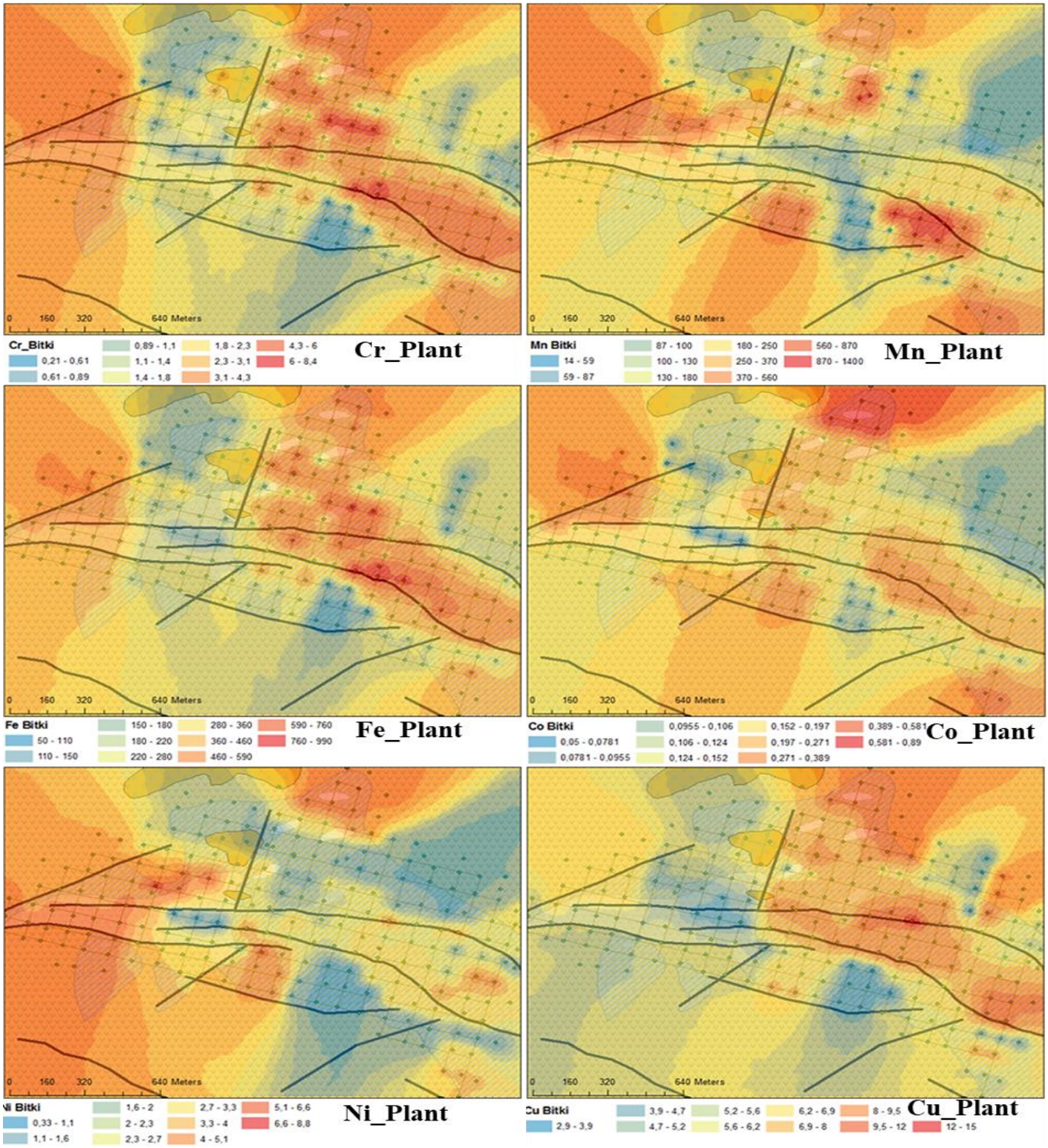

Figure 5. Spatial distribution maps of plant elements Cr, Mn, Fe, Co, Ni and Cu (Refer to Fig. 1 for geological alteration legend explanations)

The high Cd values observed near the Trabzon-Gümüşhane state highway are striking and suggest that traffic may also contribute to the high Cd values in sessile oak leaves (Fig. 6). The presence of high traffic-related Cd values in studies [e.g. 31] conducted in the region further supports this possibility.

Areas with high Sb element concentrations are observed in the southeastern and central parts of the field. High-value Sb (up to in the range of 630–1200 ppb in the southeastern and up to in the range of 1200–2400 ppb in the central part) areas are particularly striking in areas with argillic alteration and tectonic faults (Fig. 6). The areas in question are also the areas that show high concentration patterns for almost all elements, especially the sampling point in the central part of the field. In addition, relatively high Sb values were also detected in the area where phyllic alteration is surrounded by argillic alteration in the northeast of the field.

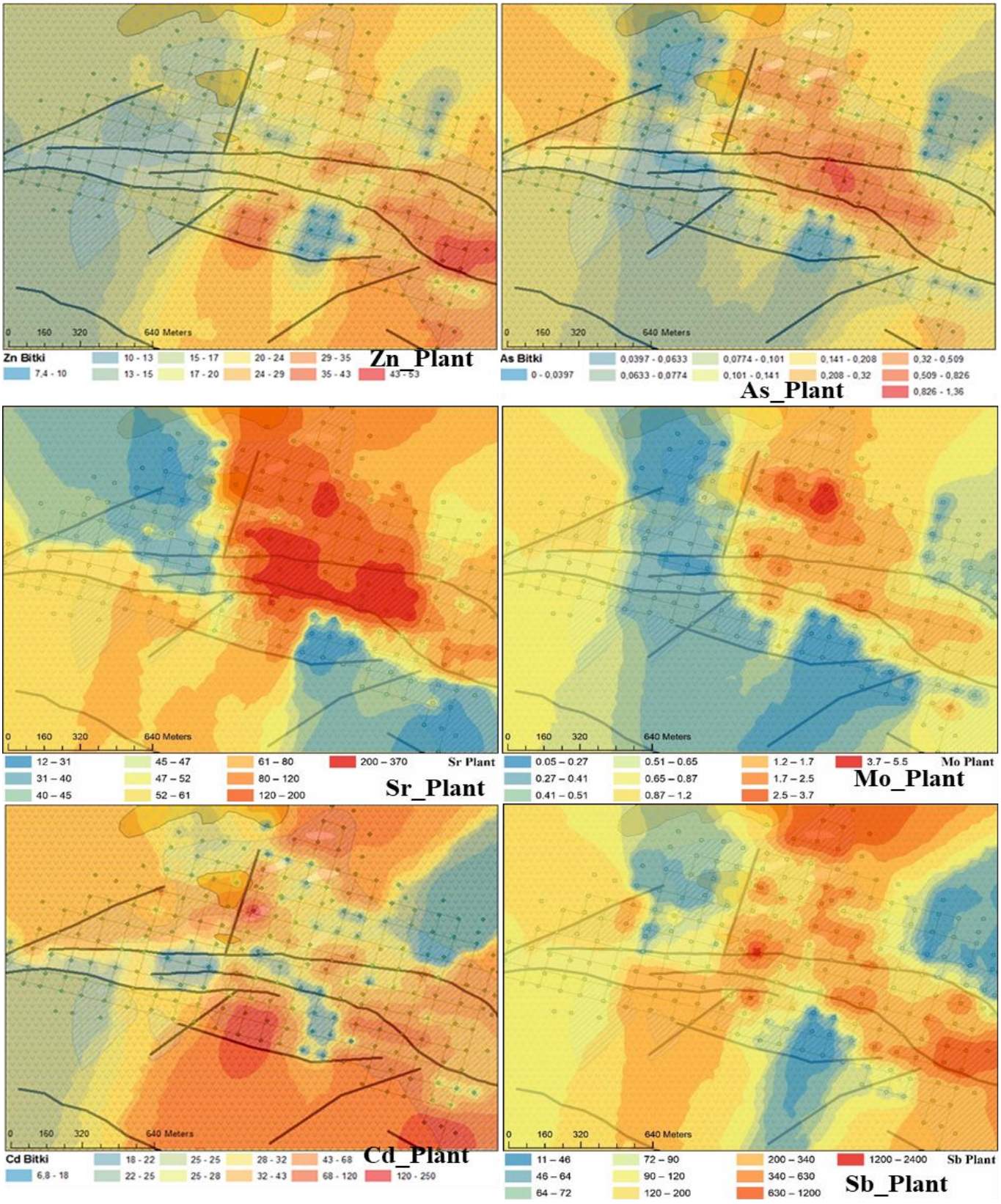

Figure 6. Spatial distribution maps of plant elements Zn, As, Sr, Mo, Cd and Sb (Refer to Fig. 1 for geological alteration legend explanations)

Barium (Ba) element concentrations exhibit high-value patterns in the east of the study area, and parallel to the tectonic fault in the middle of the study area, and again in the west of the study area in the argillic alteration and fresh rock zone associated with the tectonic fault. Ba values in the eastern part of the study area are relatively higher than other parts (Fig. 7).

Lead (Pb) concentrations in sessile oak leaves reach high values (up to 1.4–1.7 ppm) in the argillic alteration zone with intense tectonic faults in the east of the study area. Additionally, high Pb distribution areas associated with the tectonic fault have been identified in the transition zone of fresh rock-argillic alteration in the northwest of the study area (Fig. 7).

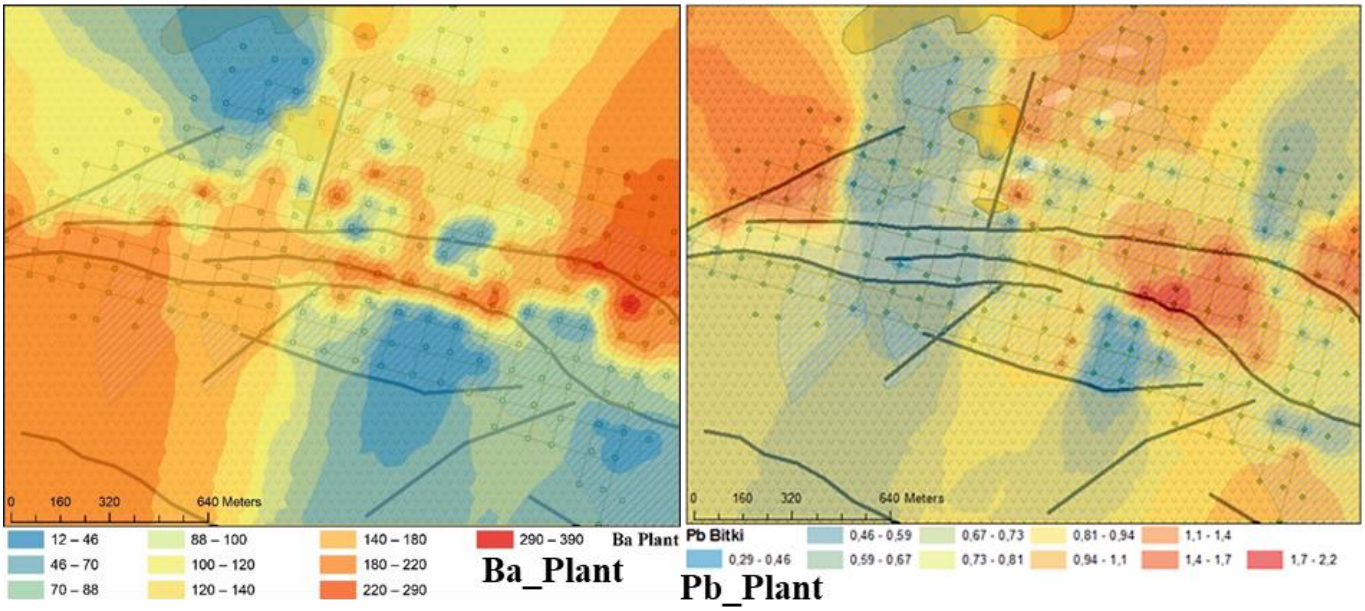

Figure 7. Spatial distribution maps of plant elements Ba and Pb (Refer to Fig. 1 for geological alteration legend explanations)

It has been observed that the concentrations of most elements in the leaves of sessile oak trees growing in the area reach high values associated with alteration and tectonic faults. When comparing the element contents of sessile oak leaves with previous studies [4,28,32,33], it has been observed that the concentrations of elements in altered sections differ from those in unaltered/fresh rock-dominant sections.

4. Conclusions

This study aimed to investigate the relationship between the concentrations of certain trace elements in sessile oak leaves and alteration zones. In this context, element analyses were performed on tree leaves collected from the Canca (Gümüşhane, Türkiye) hydrothermal alteration area. Descriptive statistical evaluations of the element concentrations in the leaves were performed. It was determined that the element concentrations in the leaves were within a wide range and above the values known for sessile oak leaves (and plants in general). Moreover, considering the median values, it was found that sessile oak leaves growing in the area were enriched with the studied trace elements. It was observed that the high element concentrations in the leaves were particularly high in the argillic zones, associated with alteration and tectonic faults (fracture zones) in the field, and that most elements reached higher concentrations compared to fresh rocks. As a result of the study, it was concluded that the element enrichments in the leaves were significantly by the elements Mo, Cu, As, Zn, and Pb, and that there was also a remarkable enrichment by the elements Cr, Mn, Co, Ni, Sb, and Ba.

Acknowledgments

This research was supported by Scientific Research Projects of TÜBİTAK under Grant Number: 113Y569. The author(s) dedicate(s) this study to the Department of Geological Engineering (Ankara Geology) on the occasion of its 90th anniversary in education (1934–2024).

References

[1] A. Vural, Investigation of the relationship between rare earth elements, trace elements, and major oxides in soil geochemistry, Environ Monit Assess, 192 (2020) 124.

[2] A. Vural, Gold and Silver Content of Plant Helichrysum Arenarium, Popularly Known as the Golden Flower, Growing in Gümüşhane, NE Turkey, Acta Phys Pol A, 132 (2017) 978–980.

[3] A. Vural, Canca (Gümüşhane) Alterasyon Sahasında Toprak ve Bitki Jeokimyası Çalışmaları ile Altın Potansiyelinin Araştırılması, Ankara, Türkiye, 2014.

[4] A. Vural, Assessment of Sessile Oak (Quercus petraea L) Leaf as Bioindicator for Exploration Geochemistry, Acta Phys Pol A, 130 (2016) 191–193.

[5] G. Kırat, N. Aydın, Pb-Zn Accumulation in Plants Grown in and Around a Pb-Zn Mine, Polish J Environ Stud, 24 (2015) 545–554.

[6] G. Kirat, N. Aydin, Phytoremediation with plants for soils polluted by boron at Akdagmadeni Pb-Zn mining district and surroundings, Yozgat, Turkey, Gazi Univ J Sci, 29 (2016) 963–970.

[7] G. Kirat, Investigation of the Biogeochemical Anomalies of Euphorbia cyparissias plant in Gümüshacıköy-Amasya Pb-Zn-Ag Deposits, Turkey, Indian J Forensic Med Pathol, 13 (2020).

[8] A. Vural, S. Kaya, N. Başaran, O.T. Songören, Anadolu Madenciliğinde İlk Adımlar, Maden Tetkik ve Arama Genel Müdürlüğü, MTA Kültür Serisi-3, Ankara, Türkiye, 2009.

[9] A. Vural, A. Kaygusuz, Geochronology, petrogenesis and tectonic importance of Eocene I-type magmatism in the Eastern Pontides, NE Turkey, Arab J Geosci, 14 (2021) 467.

[10] A. Vural, A. Kaygusuz, Petrographic and geochemical characteristics of late Cretaceous volcanic rocks in the vicinity of Avliyana (Gümüşhane, NE Turkey), J Eng Res Appl Sci, 10 (2021) 1796–1810.
[11] G. Topuz, R. Altherr, W. Siebel, W.H. Schwarz, T. Zack, A. Hasözbek, M. Barth, M. Satir, C. Şen, Carboniferous high-potassium I-type granitoid magmatism in the Eastern Pontides: The Gümüşhane pluton (NE Turkey), Lithos, 116 (2010) 92–110.
[12] A. Kaygusuz, Geochronological age relationships of Carboniferous Plutons in the Eastern Pontides (NE Turkey), J Eng Res Appl Sci, 9 (2020) 1299–1307.
[13] G. Topuz, R. Altherr, W.H. Schwarz, A. Dokuz, H.P. Meyer, Variscan amphibolite-facies rocks from the Kurtoğlu metamorphic complex (Gümüşhane area, Eastern Pontides, Turkey), Int J Earth Sci, 96 (2007) 861–873.
[14] M. Eren, Gümüşhane-Kale Arasının Jeolojisi ve Mikrofasiyes incelemesi, Karadeniz Teknik Üniversitesi, 1983.
[15] S. Pelin, Alucra (Giresun) Güneydoğu Yöresinin Petrol Olanakları Bakımından Jeolojik İncelenmesi, Karadeniz Teknik Üniversitesi, 1977.
[16] S. Tokel, Stratigraphical and volcanic history of Gümüşhane region, 1972.
[17] A. Kaygusuz, W. Siebel, C. Şen, M. Satir, Petrochemistry and petrology of I-type granitoids in an arc setting: the composite Torul pluton, Eastern Pontides, NE Turkey, Int J Earth Sci, 97 (2008) 739–764.
[18] A. Kaygusuz, Torul ve çevresinde yüzeylenen kayaçların petrografik ve jeokimyasal incelenmesi, Doktora Tezi, Karadeniz Teknik Üniversitesi, Trabzon, 227s, 2000.
[19] Ç. Saydam Eker, Petrography and geochemistry of Eocene sandstones from eastern Pontides (NE TURKEY): Implications for source area weathering, provenance and tectonic setting, Geochemistry Int, 50 (2012) 683–701.
[20] A. Kaygusuz, M. Öztürk, Geochronology, geochemistry, and petrogenesis of the Eocene Bayburt intrusions, Eastern Pontide, NE Turkey: implications for lithospheric mantle and lower crustal sources in the high-K calc-alkaline magmatism, J Asian Earth Sci, 108 (2015) 97–116.
[21] İ. Temizel, E. Abdioğlu Yazar, M. Arslan, A. Kaygusuz, Z. Aslan, Mineral chemistry, whole-rock geochemistry and petrology of Eocene I-type shoshonitic plutons in the Gölköy area (Ordu, NE Turkey), Bull Miner Res Explor, 157 (2018) 121–152.
[22] I. Temizel, M. Arslan, C. Yücel, E. Abdioğlu Yazar, A. Kaygusuz, Z. Aslan, Eocene tonalite–granodiorite from the Havza (Samsun) area, northern Turkey: adakite-like melts of lithospheric mantle and crust generated in a post-collisional setting, Int Geol Rev, 62 (2020) 1131–1158.
[23] A. Kaygusuz, A. Arslan, W. Siebel, C. Şen, Geochemical and Sr-Nd Isotopic Characteristics of Post-Collisional Calc-Alkaline Volcanics in the Eastern Pontides (NE Turkey), Turkish J Earth Sci, 20 (2011) 137–159.
[24] A. Vural, Hidrotermal Alterasyona Bağlı Element Kirliliği : Canca (Gümüşhane - Türkiye), J Investig Eng Technol, 5 (2022) 87–103.
[25] A. Vural, G. Külekçi, Zenginleştirilmiş Jeoturizm Güzergahı:Gümüşhane-Bahçecik Köyü, Euroasia J Math Eng Nat Med Sci, 8 (2021) 1–23.
[26] B. Karayigit, N. Colak, F. Ozogul, A. Gundogdu, H. Inceer, N. Bilgiçli, F.A. Ayaz, The biogenic amine and mineral contents of different milling fractions of bread and durum wheat (Triticum L) cultivars, Food Biosci, 37 (2020) 100676.
[27] A. Kurt, N. Colak, A.. Bengu, A. Gundogdu, E. Akpinar, S. Hayirlioglu-Ayaz, F.A. Ayaz, A nutritional evaluation of the berry of a new grape: "Karaerik" (Vitis vinifera L), Int J Food Stud, 7 (2018) 98–116.
[28] J.Y. Park, S.H. Jeon, J.N. Kim, H.T. Chon, A biogeochemical orientation study in Mo skarn deposits, Jecheon district in Korea, J Geochemical Explor, 146 (2014) 9–16.
[29] D.G. Krige, A stastical Approach to Some Basic Mine Valuation Problems on the Witwatersrand, J Chem Metall Soc South Min Africa, 52 (1951) 119–139.
[30] G. Matheron, Principles of geostatistics, Econ. Geol., 58 (1963) 1246–1266.
[31] A. Vural, Assessment of Heavy Metal Accumulation in the Roadside Soil and Plants of Robinia pseudoacacia, in Gumushane, Northeastern Turkey, Ekoloji, 22 (2013) 1–10.
[32] C. Anjos, C.M.F. Magalhaes, M.M. Abreu, Metal (Al, Mn, Pb and Zn) soils extractable reagents for available fraction assessment: Comparison using plants, and dry and moist soils from the Braçal abandoned lead mine area, Portugal, J Geochemical Explor, 113 (2012) 45–55.
[33] H. Turan, Z. Özdemir, S. Zorlu, Çiftehan (Ulukışla-Niğde) Bölgesinin Biyoeokimyasal Anomalilerinin Araştırılması, İstanbul Üniversitesi Mühendislik Fakültesi Yerbilim Derg, 19 (2006) 131–140.